J Mater Sci (2010) 45:4846–4850
DOI 10.1007/s10853-010-4484-6

ULTRAFINE GRAINED MATERIALS

Effect of rolling temperature on the evolution of defects and properties of an Al–Cu alloy

V. Subramanya Sarma · W. W. Jian · J. Wang · H. Conrad · Y. T. Zhu

Received: 5 March 2010 / Accepted: 5 April 2010 / Published online: 20 April 2010

Abstract The defects and properties of a precipitation hardening Al–Cu alloy 2017 were studied after rolling at room temperature (RT) and cryogenic (liquid N_2) temperature (CT). It is found that CT rolling produced practically the same hardness as RT rolling for a wide range of rolling strains. However, electrical resistivity measurement revealed a clear difference indicating different defect structures in the CT- and RT-rolled samples. This difference led to higher hardness, after subsequent ageing, for samples processed by CT rolling. It is deduced that precipitation occurred during RT rolling, which compensated for the effect of lower dislocation density (evaluated from X-ray diffraction) in RT-rolled sample, and consequently resulted in similar hardness in both RT- and CT-rolled samples. It is noted that after ageing, CT-rolled sample has higher strength ($\sim$35%) than the standard T4 treatment.

Introduction

In recent years there is a considerable scientific/technological interest in bulk ultrafine grained (UFG)/nanostructured (NS) materials due to significant improvements in mechanical properties. Bulk UFG/NS materials are usually produced in the top–down approach by severe plastic deformation (SPD) processes such as equal channel angular pressing, high pressure torsion, accumulative roll bonding, and severe cold rolling [1–14]. Severe rolling processes are particularly attractive for commercial applications because: (a) there is no necessity for special equipment/tooling and (b) ease of upscaling. Deformation (rolling) at cryogenic (liquid N_2) temperature has been shown to produce UFG/NS microstructures due to the suppression of dynamic recovery [5–12, 15–18]. Precipitation hardening Al alloys (2XXX, 6XXX, and 7XXX series) are an important class of materials due to their technological importance. It has recently been shown that these alloys offer possibilities for achieving high strength and ductility through innovative nanostructuring approach through SPD and subsequent heat treatment [11, 12, 16, 19]. Recent studies indicate that the SPD processing at room temperature (RT) of precipitation hardening Al–Mg–Si alloy (in supersaturated condition) resulted in strain-induced precipitation of second phase particles due to the large number of defects generated during deformation and consequently higher density of nucleation sites [20, 21]. Precipitate dissolution during SPD processing of an Al–Cu alloy (in two phase microstructure) and altering of the precipitation sequence during subsequent ageing were also reported [22]. The phenomenon of strain-induced precipitation during SPD processing results in less solute being available for precipitation during the subsequent ageing treatment. This is important because ageing following SPD processing results in precipitation strengthening, which counteracts any loss in strength due to reduction in dislocation density through recovery. This leads to simultaneous increase in strength and ductility [11, 12, 16, 17]. It is suggested that cryogenic deformation could prevent strain-induced precipitation due to reduced diffusivity [20].

Rolling is a common and cost effective industrial deformation technique, which can be performed at cryogenic temperature (CT), RT and elevated temperatures.

V. S. Sarma (✉)
Department of Metallurgical and Materials Engineering, Indian Institute of Technology Madras, Chennai 600 036, India
e-mail: vsarma.iitm@gmail.com; vsarma@iitm.ac.in

V. S. Sarma · W. W. Jian · J. Wang · H. Conrad · Y. T. Zhu
Department of Materials Science and Engineering, North Carolina State University, Raleigh, NC 27695, USA

However, CT rolling costs more than RT rolling, and can be justified only when it produces significantly improved mechanical properties. The present work was undertaken to evaluate if CT rolling has advantage over RT rolling for the Al–Cu alloy 2017. Specifically, we investigated the evolution of defects (e.g. precipitates and dislocation density) during severe CT and RT rolling by means of hardness, electrical resistivity and X-ray analysis. It is difficult to characterize strain-induced precipitation following SPD processing using transmission electron microscopy (TEM) because the 2017 alloy ages naturally at RT during the time consuming sample preparation and TEM observation. In contrast, electrical resistivity is very sensitive to defect densities and precipitation and can be measured within seconds of rolling, which avoids the effect of natural ageing induced structural changes. Therefore, measurement of changes in resistivity during rolling is a unique and powerful tool to characterize defect densities and to correlate with the mechanical properties.

Experimental details

Aluminium alloy 2017 (Al–4Cu–1Mn–0.5 Mg) (in wt%) was procured in the form of 2-mm thick sheets in T4 condition. Strips (20-mm wide, 50-mm long) of samples were cut from the sheet and solution treated at 500 °C for 1 h and water quenched. Immediately after quenching, the sheets were rolled at room temperature (RT rolling) and CT (liquid N_2 temperature, CT rolling) in a laboratory rolling mill to a strain of $\sim$2 in multiple passes ($\sim$5–10% reduction per pass) and samples were taken at different strains for study of microstructure/mechanical properties. For cryogenic rolling, the rolls were cooled with liquid N_2 and after each pass (reduction per pass was $\sim$5%) the sample was cooled in liquid N_2 before the next pass. Resistivity was measured at ambient temperature using a Hocking AutoSigma 2000 conductivity meter. This device works on the principle of eddy currents and is widely used for non-destructive evaluation of aerospace structures [23]. Microhardness measurements were performed on a Buehler microhardness tester at a load of 100 g for 10 s. X-ray diffraction (XRD) scans were carried out on a Rigaku D/Max diffractometer operating at 25 kV. The experimental X-ray peaks were corrected for instrumental broadening (the instrumental profile was measured on the same alloy sample annealed at 500 °C for 1 h) using FOURYA program [24]. Dislocation densities were evaluated using the modified Williamson–Hall method [25]. It may be noted that all of the measurements (hardness, resistivity and XRD) were carried out at RT, i.e. measurements on the cryorolled samples were taken after they reached RT.

Results and discussion

The microstructure following solutionizing treatment is shown in Fig. 1. The average grain intercept length in the solutionised condition was found to be $\sim$50 μm. Figure 2a shows the variation of hardness with rolling strain ($\varepsilon = \ln(t/t_0)$), where 't' is the final thickness and 't_0' is the starting thickness, i.e. 2 mm) following CT and RT rolling of 2017 alloy. The hardness increase with strain can be divided into two regions (Fig. 2a), the region 1 in which the rate of increase is relatively high up to a strain of 0.5, and the region 2 (at rolling strains >0.5) in which there is a significantly reduced strain hardening. The straight lines are drawn only to illustrate the differences in the rate of hardness increase in both regions. It can be seen that the effect of cryogenic rolling on the hardness of both samples is not very significant at rolling strains >1. However, it should be noted that these hardness values in Fig. 2a are $\sim$35% higher than that obtained after the conventional T4 treatment (T4 results in hardness of $\sim$1,300 MPa).

Figure 2b shows the variation of the resistivity with rolling strain in the 2017 alloy during RT and CT rolling. The significant finding from Fig. 2b is that samples processed by RT rolling have clearly lower resistivity than the samples processed by CT rolling. This suggests that the defect structures in the RT-rolled samples differ from those in the CT-rolled sample despite the nearly identical microhardness values shown in Fig. 1a. However, similar to the hardness variation with strain in Fig. 2a, the resistivity changes also show two regions and the transition occurs at $\sim$0.5. In region 1, resistivity increases at a faster rate up to a strain of 0.5; in region 2, the resistivity increases at a much smaller rate. The resistivity value at zero strain corresponds to the value after the solutionising and quenching treatment and measurement was taken just before rolling.

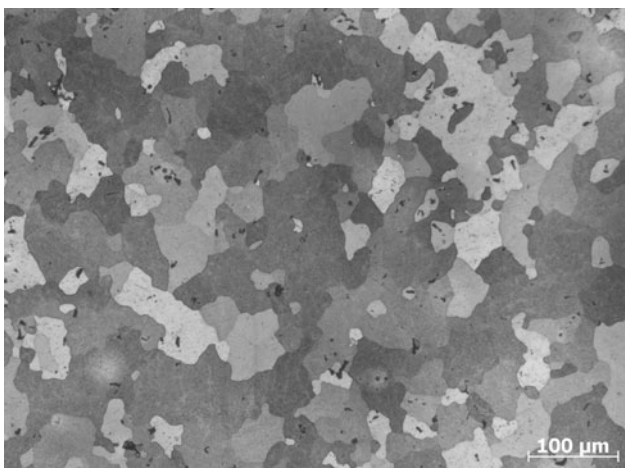

Fig. 1 Microstructure of AA2017 alloy following solutionizing at 500 °C for 1 h

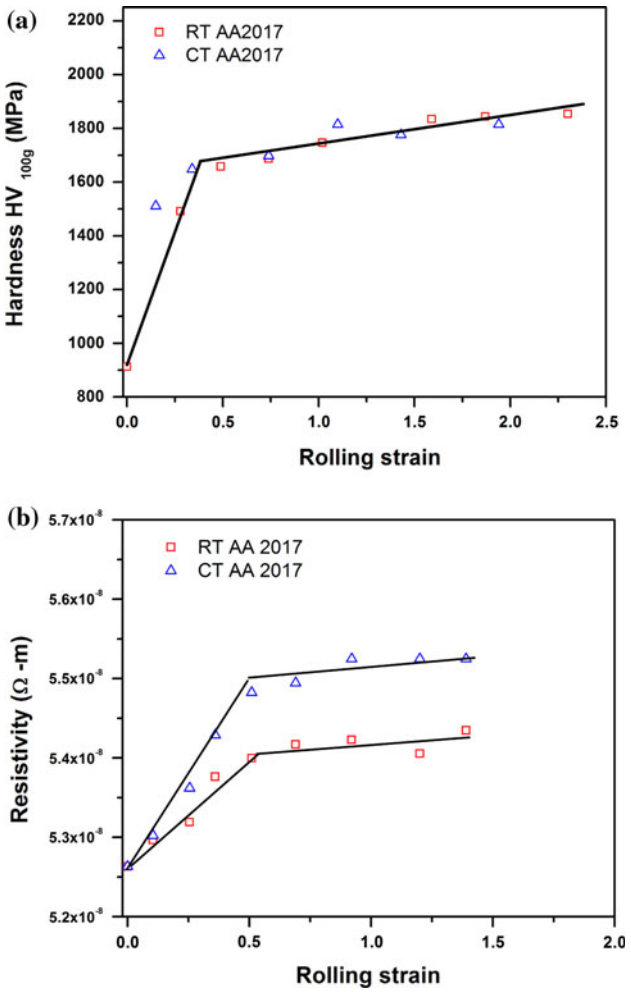

Fig. 2 **a** Variation of hardness and **b** resistivity with rolling strain in 2017 alloy after and RT rolling and CT rolling at liquid N_2 temperature

An increase in resistivity during deformation generally results from an increase in dislocation density. However, resistivity also changes with the precipitation of second phases. The precipitation sequence during ageing of Al alloys is very complex and is specific to the alloy system/composition. In Al–Cu alloys, the precipitation sequence involves many intermediate steps, i.e. GP zones → $\theta'' \rightarrow \theta'$, before the equilibrium phase θ is formed. Formation of solute clusters/GP zones increases the resistivity and formation of equilibrium precipitates results in the lowering of resistivity during ageing [26]. The increase in resistivity during CT/RT rolling of 2017 could be attributed to an increase in dislocation density. However, a significantly lower increase in resistivity in RT rolled-2017 when compared with CT sample is more likely due to precipitation of second phases during deformation.

The other factor that could result in a lower increase in resistivity between CT and RT rolling is a lower dislocation density following RT rolling. However, this is unlikely the primary cause for the observations in Fig. 2 because a significantly lower dislocation density following RT rolling would have resulted in a significantly lower hardness/strength values and clearly this is not seen (Fig. 2a). Precipitation of second phases other than G–P zones decrease the overall resistivity of the alloy and this counteracts the increase in resistivity due to generation of dislocations during rolling. It is therefore concluded that the strain-induced precipitation contributes to the lower rate of increase in resistivity with strain (Fig. 2b). However, at the same time, it also contributed to higher hardness, as is discussed below.

It is well established that Al–Cu alloys following solution treatment and quenching are unstable and decompose at RT with G–P zones forming easily during short-time exposure to RT. This is observed from the significant increase in resistivity from 5.0×10^{-8} Ω m following quenching to 5.25×10^{-8} Ω m within an hour of storage at ambient temperature. Therefore, the microstructure in Al–Cu alloy before rolling is expected to consist of G–P zones and the supersaturated matrix. During rolling at RT, the G–P zones could transform to other intermediate phases and thereby contribute to reduced resistivity. The SPD processing has been shown to accelerate the precipitation kinetics and also affect the precipitation sequence and morphology [12, 17, 22, 27]. It is proposed that the change in morphology of the precipitates (predominantly spherical as opposed to rods/plates) is attributed to strain-induced precipitation and shearing of these precipitates during continued deformation [20, 21, 27]. The transformation of GP zones to "θ" could be assisted by the high dislocation density/vacancies which are generated by cold rolling. The dislocations act as nucleation sites because the strain field of the dislocation is able to reduce the misfit between the parent and product phases [28]. Study of changes in lattice parameter can also throw light on precipitation events [29]. We tried to evaluate the lattice parameter of the rolled samples using Nelson–Riley plot but there was lot of scatter in the data and the fits were very poor. The scatter could be due to residual stresses present following severe cold rolling.

We present here indirect evidence of precipitation during RT rolling through ageing studies on rolled samples. If strain-induced precipitation/growth occurred during rolling, then lower amount of solute should be available for precipitation during the subsequent ageing treatment. To check this, ageing treatments were carried out at 100 °C. The hardness variation as a function of ageing time is shown in Fig. 3. There is an initial decrease in hardness following ageing for 2 h and subsequently hardness increases marginally. The hardness in RT-rolled sample is consistently lower than that of CT-rolled sample (except after 2 h and this could be due to higher dislocation

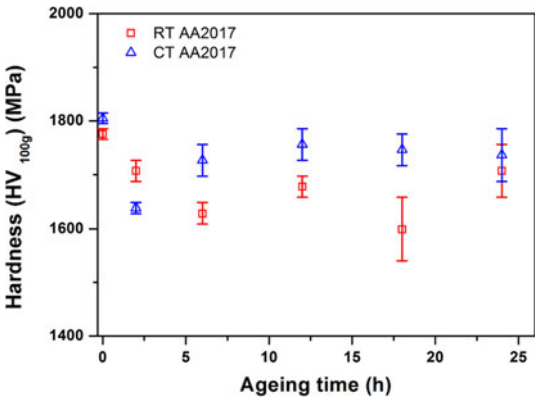

Fig. 3 Variation of hardness following ageing (at 100 °C) of RT- and CT-rolled 2017 alloy

recovery rate in CT alloy) indicating that the contribution to strength from precipitation strengthening is lower in the RT-rolled alloy. The above result is consistent with the resistivity studies and indicate that strain-induced precipitation occurs in the 2017 alloy during RT rolling. From the empirical equation, yield flow stress, $\sigma = H_V/3$, one can see that the following cold rolling and ageing, strengths of $\sim$600 MPa can be obtained which is $\sim$35% higher than that obtained after the T4 treatment (425 MPa) in this alloy [30].

From the specific dislocation resistivity '$\Re$' (for Al it is $3 \pm 1\ \Omega\ m^3$ [31]), the dislocation densities at different rolling strains was estimated by using the relation $(\rho_e - \rho_0)/\Re$, where 'ρ_e' is the resistivity at a given strain and 'ρ_0' is the resistivity in the solutionised condition (measured just before rolling) (Fig. 4a). Dislocation densities were also determined from X-ray diffraction peaks using the modified Williamson–Hall (W–H) method and plotted in Fig. 4b. In the modified W–H method, (ΔK) is plotted against $KC^{0.5}$ ($\Delta K = 2B\mathrm{Cos}(\theta_B)/\lambda$, $K = 2\mathrm{Sin}(\theta_B)/\lambda$), where '$B$' is the full width at half maximum of the strain broadened $\{hkl\}$ peak, 'θ_B' is the Bragg angle of the corresponding $\{hkl\}$ peak, 'λ' in the wave length of the X-rays (0.15046 nm for Cu target used in the present study) and 'C' is the average dislocation contrast factor to account for the strain anisotropy [32]. The 'C' values were calculated using the elastic constants assuming that all the slip systems are equally populated and the edge and screw dislocations are equally probable [33]. Figure 5 shows a typical plot of ΔK versus $KC^{0.5}$ for CT- and RT-rolled 2017 alloy rolled to a strain of 2. The slope obtained from the linear fit to the data is related to the microstrain and in turn to the dislocation density in the material as $\sqrt{\pi/2}Ab\sqrt{\rho_d}$, (where '$A$' is constant depending on the effective outer cut off radius of dislocations and taken as 0.63, 'b' is the burgers vector of dislocation (0.286 nm for Al), 'ρ_d' is the dislocation density) [34]. The dislocation densities estimated from X-ray diffraction in CT- and

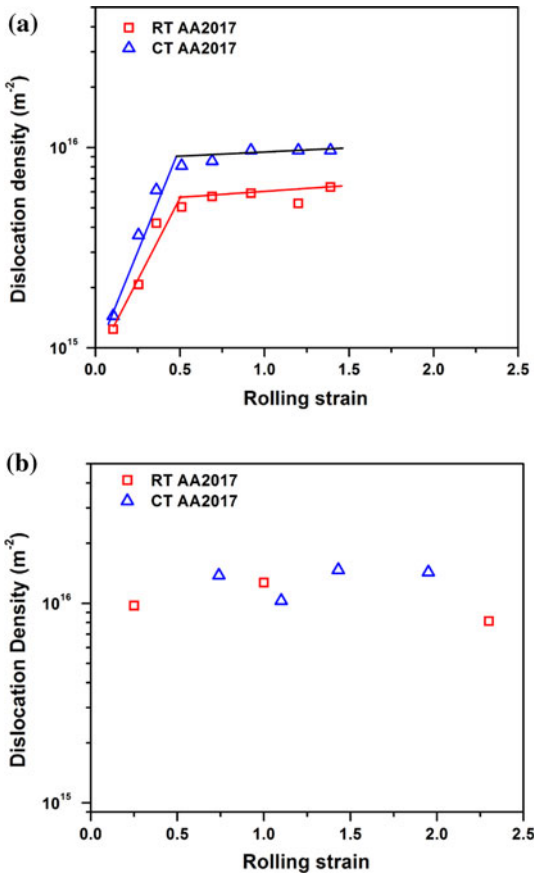

Fig. 4 Variation of dislocation density with rolling strain determined from **a** electrical resistivity and **b** X-ray diffraction analysis

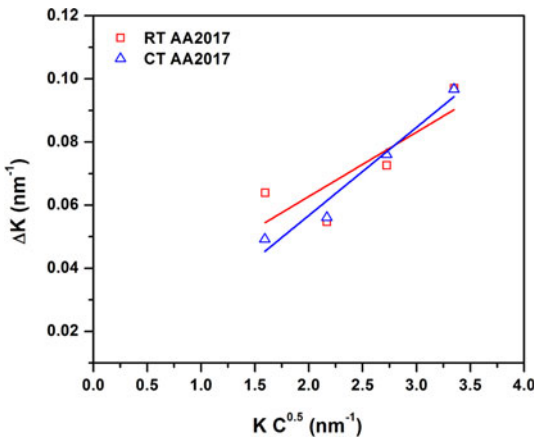

Fig. 5 Modified Williamson–Hall plot for CT- and RT-rolled 2017 alloys (strain $\sim$2)

RT-rolled 2017 alloy are in the range of $1 \times 10^{16}\ m^{-2}$ and RT-rolled sample has slightly lower dislocation density ($\sim$10–15%) when compared to CT-rolled sample. The dislocation density obtained from resistivity measurement compares reasonably well with that obtained from XRD analysis in CT-rolled sample.

From the above experimental results on dislocation densities and electrical resistivity, it can be deduced that RT rolling produced a lower dislocation density than CT rolling, but RT rolling also produced precipitation while CT rolling did not produce precipitation. Both precipitation and lower dislocation density led to lower electrical resistivity in the RT-rolled samples, as shown in Fig. 1b. The effect of the precipitation on hardness appeared to cancel the effect of lower dislocation density on hardness as shown in Fig. 2a. Hardening caused by precipitation should increase the strength of the RT-rolled sample. On the other hand, the lower dislocation density should result in lower strength, according to the classical Taylor relation, $\sigma = \alpha G b \sqrt{\rho_d}$, where α is constant depending on dislocation arrangement ($\sim$0.5–1), 'G' is shear modulus, 'b' is magnitude of the burgers vector and 'ρ_d' is the dislocation density. The net result of these two opposing effects led to the same hardness in the RT- and CT-rolled samples.

Conclusions

Studies on hardness and defects (by electrical resistivity and X-ray diffraction measurements) of CT- and RT-rolled 2017 alloy, lead to following conclusions:

(1) There is no significant enhancement of hardness in 2017 alloys due to CT rolling vis-à-vis RT rolling. There is a, however, significant increase in strength ($\sim$35%) when compared to the hardness obtained after the standard T4 temper.
(2) The resistivity of RT-rolled sample is lower than that of CT-rolled sample. This is attributed to the strain-induced precipitation as well as lower dislocation density produced in the samples deformed by RT rolling.
(3) The strain-induced precipitation is believed to contribute to the strength in RT-rolled sample, which compensated for the softening caused by lower dislocation density. This precipitation resulted in similar hardness in both RT- and CT-rolled 2017 samples.
(4) Strain-induced precipitation in RT-rolled sample was verified by post ageing treatment which showed a lower increase in hardness in RT-rolled sample when compared to CT-rolled sample.

Acknowledgements One of the authors (VSS) acknowledges the financial support of Indo-US Science and Technology Forum (IUSSTF) through a sabbatical research fellowship. Other co-authors acknowledge the support by U.S. Army Research Office and Army Research Laboratory.

References

1. Valiev RZ, Islamgaliev RK, Alexandrov IV (2000) Prog Mater Sci 45:103
2. Valiev RZ, Langdon TG (2000) Prog Mater Sci 51:881
3. Zhilayev AP, Langdon TG (2008) Prog Mater Sci 53:893
4. Saito Y, Utsunomiya H, Suji N, Sakai T (1999) Acta Mater 47:579
5. Wang Y, Chen M, Zhou F, Ma E (2002) Nature 419:912
6. Sarma VS, Sivaprasad K, Sturm D, Heilmaier M (2008) Mater Sci Eng A 489:253
7. Xiao GH, Tao NR, Lu K (2009) Mater Sci Eng A 513–514:13
8. Lee YB, Shin DH, Park KT, Nam WJ (2004) Scr Mater 51:355
9. Rangaraju N, Raghuram T, Vamsi Krishna B, Prasad Rao K, Venugopal P (2005) Mater Sci Eng A 398:246
10. Lee TR, Chang CP, Kao PW (2005) Mater Sci Eng A 408:131
11. Zhao YH, Liao XZ, Cheng S, Ma E, Zhu YT (2006) Adv Mater 18:2280
12. Shanmugasundaram T, Murty BS, Sarma VS (2006) Scr Mater 54:2013
13. Zhu YT, Liao XZ (2004) Nat Mater 3:351
14. Valiev RZ, Alexandrov IV, Zhu YT, Lowe TC (2002) J Mater Res 17:5
15. Panigrahi SK, Jayaganthan R (2008) Mater Sci Eng A 492:300
16. Cheng S, Zhao YH, Zhu YT, Ma E (2007) Acta Mater 55:5822
17. Niranjani VL, Hari Kumar KC, Sarma VS (2009) Mater Sci Eng A 515:169
18. Humphreys FJ, Hatherly M (1996) Recrystallization and related annealing phenomena. Pergamon, Oxford
19. Zhao YH, Liao XZ, Jin Z, Valiev RZ, Zhu YT (2004) Acta Mater 52:4589
20. Roven HJ, Liu M, Werenskiold JC (2008) Mater Sci Eng A 483–484:54
21. Hockauf M, Meyer LW, Zillmann B, Heitschold M, Schulze S, Kruger L (2009) Mater Sci Eng A 503:167
22. Murayama M, Horita Z, Hono K (2001) Acta Mater 49:21
23. http://www.geinspectiontechnologies.com/download/products/ec/GEIT-50005EN_autosigma3000.pdf
24. Cheary RW, Coelho A (1996) Fourya—line profile fourier analysis program, version 4.2. http://www.ccp14.ac.uk/ccp/ccp14/ccp14-by-program/fourya-windows/
25. Ungar T, Borbely A (1996) Appl Phys Lett 69:3173
26. Esmaelli S, Poole WJ, Lloyd DJ (2000) Mater Sci Forum 331–337:995
27. Kim WJ, Kim JK, Park TY, Hong SI, Kim DI, Kim YS, Lee JD (2002) Met Mater Trans 33A:3155
28. Porter DA, Easterling KE (2004) Phase transformations in metals and alloys. Taylor and Francis, New York
29. Starink MJ, Van Mourik P (1994) J Mater Sci 29:2835. doi: 10.1007/BF01117590
30. ASM Metals Reference Book (2004) 3rd edn. ASM International, Materials Park, Ohio
31. Friedel J (1964) Dislocations. Addison-Wesley, MA
32. Ungár T, Dragomir I Révész A Borbély A (1999) J Appl Cryst 32:992
33. http://metal.elte.hu/anizc/
34. Woo W, Ungar T, Feng Z, Kenik E, Clausen B. Met Mater Trans A. doi:10.1007/s11661-009-9963-5